

# In Silico Approach To Identify Potential Thyroid Hormone Disruptors among Currently Known Dust Contaminants and Their Metabolites

Jin Zhang,<sup>†</sup> Jorke H. Kamstra,<sup>‡</sup> Mehdi Ghorbanzadeh,<sup>†</sup> Jana M. Weiss,<sup>‡,§</sup> Timo Hamers,<sup>‡</sup> and Patrik L. Andersson<sup>\*,†</sup>

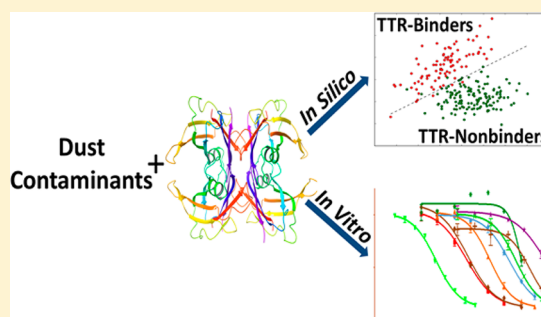
<sup>†</sup>Department of Chemistry, Umeå University, SE-901 87 Umeå, Sweden

<sup>‡</sup>Institute for Environmental Studies (IVM), VU University Amsterdam, De Boelelaan 1087, 1081 HV Amsterdam, The Netherlands

<sup>§</sup>Environmental Chemistry Unit, Department of Environmental Science and Analytical Chemistry (ACES), Stockholm University, SE-106 91 Stockholm, Sweden

## S Supporting Information

**ABSTRACT:** Thyroid hormone disrupting chemicals (THDCs) interfere with the thyroid hormone system and may induce multiple severe physiological disorders. Indoor dust ingestion is a major route of THDCs exposure in humans, and one of the molecular targets of these chemicals is the hormone transporter transthyretin (TTR). To virtually screen indoor dust contaminants and their metabolites for THDCs targeting TTR, we developed a quantitative structure–activity relationship (QSAR) classification model. The QSAR model was applied to an in-house database including 485 organic dust contaminants reported from literature data and their 433 *in silico* derived metabolites. The model predicted 37 (7.6%) dust contaminants and 230 (53.1%) metabolites as potential TTR binders. Four new THDCs were identified after testing 23 selected parent dust contaminants in a radio-ligand TTR binding assay; 2,2',4,4'-tetrahydroxybenzophenone, perfluoroheptanesulfonic acid, 3,5,6-trichloro-2-pyridinol, and 2,4,5-trichlorophenoxyacetic acid. These chemicals competitively bind to TTR with 50% inhibition (IC<sub>50</sub>) values at or below 10 μM. Molecular docking studies suggested that these THDCs interacted similarly with TTR via the residue Ser117A, but their binding poses were dissimilar to the endogenous ligand T4. This study identified new THDCs using an *in silico* approach in combination with bioassay testing and highlighted the importance of metabolic activation for TTR binding.



## INTRODUCTION

The thyroid hormone (TH) system regulates important physiological processes such as energy metabolism, brain growth and development, and reproduction.<sup>1</sup> TH homeostasis can be disturbed by thyroid hormone disrupting chemicals (THDCs) such as bromophenols and per- and polyfluoroalkyl substances (PFASs).<sup>2–4</sup> Malfunctioning of the human TH system has different adverse effects at different life stages. During embryonic development, hypothyroidism can cause central nervous system malfunctions such as visuo-spatial processing difficulties.<sup>5</sup> TH disruption may also be related to Alzheimer's disease and depression in later life stages.<sup>6,7</sup>

One of the molecular targets of THDCs is the thyroid transport proteins that facilitate the distribution of the hydrophobic THs through the blood and deliver THs to their target tissues. There are three human TH transporters: transthyretin (TTR), TH-binding globulin (TBG), and albumin. For two reasons, this work focuses on compounds interfering with TTR. First, TTR could potentially transport THDCs across protective physiological barriers such as the placenta and the blood–brain barrier, allowing them to disturb vital functions of vulnerable organs.<sup>8</sup> Second, competitive

binding of THDCs to TTR would perturb thyroid hormone levels and cause malfunctions in these organs.<sup>9</sup> It is critical to identify compounds interfering with TTR for decreasing TH-related risks presented by industrial chemicals.

The ingestion of indoor dust is a major route of THDCs exposure in humans.<sup>10,11</sup> The daily dust intake of 2.5-year-old children is estimated at 50–100 mg with a median of 60 mg, whereas that of adults is estimated to be 0.56–100 mg with a median of 30 mg.<sup>12</sup> In another study, worst case daily dust intakes of around 20 and 200 mg were estimated for adults and toddlers, respectively.<sup>10</sup> THDCs in household dust mainly originate from (1) consumer goods (including personal care products) and building materials and (2) outdoor environments.<sup>13</sup> Chemicals added to consumer goods can be transferred to indoor dust by molecular diffusion or as particulates via wear and tear. An additional pathway is molecular or particulate deposition from ventilation systems

Received: April 7, 2015

Revised: July 15, 2015

Accepted: July 24, 2015

Published: July 24, 2015

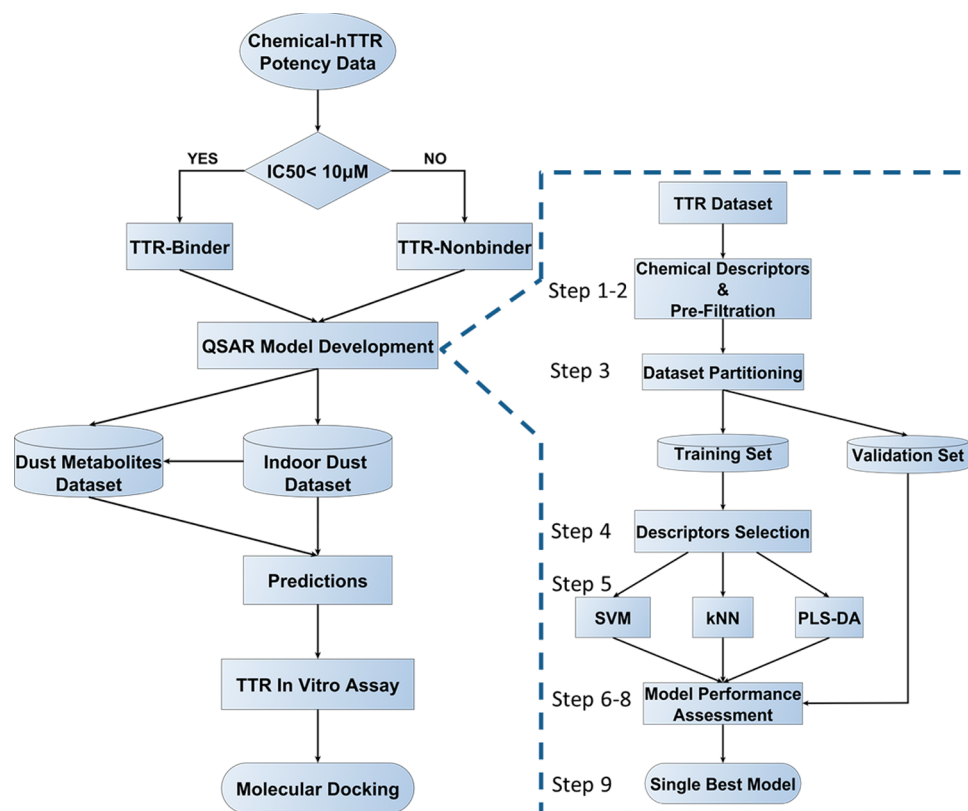


**Figure 1.** Protocol for thyroid hormone disruptor chemical identification adopted in this study with details of the stepwise model development process, the *in vitro* assay, and the molecular docking investigations on ligand–protein interactions.

that transport chemicals indoors from the outdoor environment. Major chemical groups in household dust include flame-retardants (e.g., polybrominated diphenylethers (PBDEs)), pesticides, plasticizers (e.g., phthalates) and classical persistent organic pollutants (POPs) (e.g., polychlorinated biphenyls (PCBs)), and PFASs.<sup>14</sup>

The ingested THDCs (e.g., PBDEs) might be biotransformed via metabolism.<sup>15</sup> The addition of a reactive and polar group during Phase I metabolism does not necessarily detoxify xenobiotic compounds and may actually increase their toxicity via bioactivation. For example, the hydroxylation of PCBs and PBDEs by cytochrome P450 (CYP) mono-oxygenases significantly increases their TTR potency, resulting in biotransformed derivatives that bind more strongly to TTR than does its native ligand thyroxine (T4).<sup>16–19</sup> In addition, the levels of such metabolites in the human circulation can be considerable and even comparable to those of their parent compounds in some populations.<sup>20,21</sup> It is therefore important to consider metabolic activation when screening industrial chemicals for their thyroid hormone disrupting capacities.

*In silico* approaches are able to assess the potential toxicity of chemicals fast and cost-efficiently. Two commonly used *in silico* methods are quantitative structure–activity relationship (QSAR) modeling and molecular dockings. In QSAR modeling, a set of predictor variables (chemical descriptors) is related to one or several response variables (biological or toxicological activity). QSAR models can be based on continuous or binary activity data, and models based on binary data can be used to classify chemicals as either active or inactive. Such models have been developed to predict biodegradability and narcotic effects in fish and to prioritize hits for further testing.<sup>22–24</sup> Molecular

docking is a useful tool to study potential ligand–protein bonding interactions.

In this study, we present a protocol to identify and study new THDCs combining QSARs and molecular docking techniques combined with experimental studies. The study focus on organic contaminants potency to disturb hormonal transport by TTR; however, it is well-known that exogenous compounds may disturb other critical TH related pathways. The QSAR classification model was applied to an in-house database of indoor dust contaminants and their potential metabolites aiming to predict their potency for interfering with T4–TTR binding (Figure 1). A set of 23 environmental relevant dust contaminants was selected and tested in a radio-ligand TTR binding assay aiming at identifying novel TTR binders and evaluating the developed model. Molecular level interactions with TTR of the identified binders were further studied using molecular docking.

## MATERIALS AND METHODS

The protocol was developed in a stepwise procedure (Figure 1): (1) calculating chemical descriptors, (2) prefiltering descriptors based on their variation, (3) partitioning of the TTR data set into training and validation sets, (4) selecting the statistically most significant descriptors, (5) developing models using the training set, (6) externally validating the model using the validation set, (7) defining applicability domain, (8) calculating performance statistics, and (9) selecting the best model and predicting the outcome of nontested chemicals. Details on each of these nine steps are given below together with details on the in-house databases, bioassay testing, and molecular modeling.

**TTR Data Set.** We retrieved data on competitive binding to human TTR from the work of Weiss et al. (Table S1).<sup>25</sup> Only binding data to human TTR were considered since human exposure is the focus of this study. By this means, we also avoid species-related variation, as this is an important aspect due to variable binding efficiency between species; e.g., T4 has a higher affinity for mammalian TTR than for amphibian or bird TTR, while the opposite is true for triiodothyronine (T3).<sup>16</sup> The chemicals were classified as binders if the concentration at 50% inhibition (IC<sub>50</sub>) for their interaction with TTR was 10  $\mu$ M or below and as nonbinders otherwise. The cutoff value of 10  $\mu$ M was chosen to be conservative and to limit the identification of false positives. Most of the compounds in the data set are hydrophobic and have low water solubility, and their experimentally determined IC<sub>50</sub> values may be unreliable if they were determined at concentrations close to their solubility range. The final TTR data set of 222 unique compounds (88 binders and 134 nonbinders) was used as the input for model development. The majority of data (190 out of 222) were produced using a radio-ligand TTR binding assay (data derived from other assays were marked in Table S1).<sup>19</sup> No particular pattern in the data related to source was seen in the modeling, and thus, all data was merged. TTR has two binding sites, one with high affinity and a second with 2 orders of magnitude lower affinity. The combined data set includes data that may represent interactions at both the high-affinity and the lower affinity binding sites on TTR.

**Indoor Dust Data Set.** A database of organic chemicals identified in indoor dust was compiled on the basis of the set presented by Mercier et al.<sup>14</sup> Additionally, we collected data reported in PubMed (<http://www.ncbi.nlm.nih.gov/pubmed>) and ScienceDirect (<http://www.sciencedirect.com/>) from Jan 1, 2010 to Oct 30, 2014 by performing searches using different combinations of the keywords “indoor”, “household”, “dust”, and “chemical”. The molecular structures of the dust chemicals were downloaded from SciFinder (<http://www.cas.org/products/scifinder>). The indoor dust data set can be found in Table S2.

**Metabolite Data Set.** The potential metabolites of the dust contaminants were proposed by using MetaSite v4.1 under the “Liver” setting, which predicts the effects of metabolic transformations mediated by the CYP isoenzymes CYP2C9, CYP2D6, and CYP3A4.<sup>26</sup> The software first locates potential sites for metabolic transformation on each compound by predicting the interactions between enzyme and compound. A list of biotransformation rules are then applied to these sites to generate a set of potential Phase I metabolites that are ranked on the basis of their likelihood for tissue accumulation. For each parent dust compound, the metabolite with the highest ranking score was added into a new data set entitled dust metabolite data set.

**Calculation of Molecular Descriptors and Prefiltration.** Before computing molecular descriptors, we processed the structures of the chemicals in the three studied data sets (TTR binders/nonbinders, indoor dust contaminants, and their metabolites) with ChemAxon JChem Standardizer,<sup>27</sup> using the “Add explicit hydrogens”, “Aromatize”, “Clean 2D”, and “Remove fragment” settings. After this preprocessing, 188 2D descriptors were calculated for each compound using the Molecular Operating Environment (MOE) software package.<sup>28</sup> Descriptors with low variation (i.e., if 70% of the values are constant) were removed, as they would not influence the model significantly, which reduced the number of descriptors to 132.

**Data Set Partitioning.** The Kennard-Stone algorithm was used to split the TTR data set into a training set for model development containing 80% of the compounds and a validation set for model validation.<sup>29</sup> To ensure that both subsets had the same ratio of predicted active and predicted inactive compounds, the algorithm was applied to binders and nonbinders, respectively. The training/validation sets were created by merging the chemicals selected by the algorithm as training/validation compounds in both activity classes. The partitioning resulted in a training set of 178 compounds and a validation set of 44 compounds. Details of the Kennard-Stone algorithm are given in the Supporting Information.

**Descriptor Selection and Correlation Analysis.** The Mutual Information-Differential Shannon Entropy (MI-DSE) approach was developed to identify the descriptors with the greatest amount of class-specific information for the class-imbalanced data set.<sup>30</sup> The calculations were done in Python (version 2.7.5), and details of the MI-DSE calculations are given in the Supporting Information. The 132 prefiltered descriptors were first ranked on the basis of their MI-DSE scores followed by a correlation analysis. Among highly correlated pairs of descriptors (i.e., those with correlation coefficients above 0.85), descriptors with the lower MI-DSE scores were deleted and not considered for the final set of descriptors.

**QSAR Modeling Methods.** The k Nearest Neighbor (kNN), Partial Least Squares-Discriminant Analysis (PLS-DA), and C-SVC from a Library for Support Vector Machines (LIB-SVM) algorithms were used to build three different models for classifying compounds as binders or nonbinders. PLS-DA and kNN were calculated using the classification tool box with MATLAB R2014a,<sup>31</sup> and LIB-SVM was performed in KNIME 2.9.2.<sup>32</sup> Details of these algorithms are given in the Supporting Information.

**Model Statistics and Applicability Domain.** Model performance was evaluated by leave-one-out (LOO) cross-validation (internal validation) and by using a validation set for external validation. Three parameters were calculated to quantify the models' predictive abilities: the correct classification rate (CCR), specificity (SP), and sensitivity (SN). The equations used to compute these quantities were:

$$CCR = \frac{TP + TN}{TP + TN + FP + FN} \quad SP = \frac{TN}{TN + FP} \quad SN = \frac{TP}{TP + FN}$$

where TN and TP are the number of true negatives and true positives and FN and FP are the number of false negatives and false positives, respectively. The model having the “best” performance with respect to these three parameters was used to predict the activity class of indoor dust chemicals and their major metabolites.

The Hotelling T<sup>2</sup> test was used to measure the distances between query compounds and the model center based on the descriptor space of the training set data. The resulting distances (i.e., Hotelling T<sup>2</sup> values) were used to define the applicability domain (AD). A principal component analysis (PCA) model with 5 principal components (PCs) was built on the basis of the training set by using the 132 prefiltered MOE descriptors. This model was then projected onto the data set of indoor dust chemicals and their metabolites. The 95% and 99% confidence interval values were used to define the model's applicability domain. Chemicals with Hotelling T<sup>2</sup> values outside the 95% confidence interval value were regarded as “moderate outliers”. Compounds with values outside the 99% confidence interval



value were treated as “severe outliers”, and these were excluded from further testing and predictions.

**TTR Binding Assay.** A set of 23 dust contaminants was selected to identify novel TTR binders and to evaluate the model, and these were tested in a competitive [ $^{125}\text{I}$ ]-T4-TTR ligand binding assay. Note these chemicals were not selected as an additional external validation set of the QSAR model; i.e., they were not selected to be structurally balanced and to cover the entire chemical domain, but to include a range of various household dust contaminants. The assay was performed according to the experimental procedures described in a previous study.<sup>19</sup> In short, a mixture of radio labeled [ $^{125}\text{I}$ ]-T4 (T4\*) (PerkinElmer, The Netherlands) and unlabeled T4 (Sigma-Aldrich, Germany) was incubated with purified TTR from human plasma (Sigma-Aldrich, Germany) and the competing compounds at different concentrations for at least 16 h at 4 °C in TRIS buffer (pH 8.0; 0.1 M NaCl, 0.1 mM EDTA). After incubation, the TTR-bound T4/T4\* was separated from the unbound T4/T4\* on a biogel column P-6PG (Biorad, The Netherlands). The eluate was counted on a gamma counter (LKB Wallack 1282 Compu-gamma CS). The tested compounds included 11 predicted binders and 12 predicted nonbinders (Table S8). The standard solutions of these compounds were dissolved in dimethyl sulfoxide to the initial concentrations of 1 mM. All stock solutions were diluted to the experimental concentrations right before the experiment. Dose–response curves were least-squares fitted using a nonlinear regression model (Hill equation) in GraphPad (version 5.02), yielding 50% inhibition concentrations.

**Molecular Docking.** Molecular docking studies were carried out to probe the molecular interactions between TTR and confirmed TTR binders from the assays. We selected the TTR-Tafamidis complex (PDB code: 3TCT) for the docking studies since (1) the structure is well-defined with a low resolution (1.30 Å) and a low temperature factor (16.5) of its binding pocket and (2) the coligand Tafamidis has smaller molecular volume (222 Å<sup>3</sup>) than T4 (319 Å<sup>3</sup>), which enables it to interact with residues (e.g., Ser 117) deeper inside the pocket. This allowed us to better predict the binding poses of confirmed TTR binders, which have molecular volumes smaller than T4 but similar to Tafamidis. The structure was downloaded from the RCSB Protein Data Bank (<http://www.rcsb.org/pdb/>) and prepared using the Protein Preparation Wizard from Schrödinger suite.<sup>33</sup> The grid of the ligand binding site was derived from the endogenous binding site. After conformation and tautomer generation with LigPrep,<sup>34</sup> compounds were docked into the ligand-binding pocket of the protein using the Glide module with standard precision under the OPLS 2005 Force Field formalism.<sup>35</sup> For each compound, generated docking poses were inspected and the poses with the highest score were chosen for further analysis to reveal its interactions with TTR.

## RESULTS AND DISCUSSION

**Indoor Dust and Dust Metabolites Data Set.** In total, 485 organic chemicals have been reported to be present in household dust (Table S2). This means that the number of known indoor dust contaminants has increased by 263 since the review in 2011 by Mercier et al.<sup>14</sup> The physicochemical properties of these compounds, including their hydrophobicity and molecular size, vary widely (Figure S1). In keeping with the findings of Mercier et al.,<sup>14</sup> a large share of the dust contaminants are biocides (11%), PCBs (10%), flame-

retardants (10%), PFASs (9%), and phenols (6%) (Figure S2). More recently, a range of polychlorinated dioxins and dibenzofurans, together with some of their brominated analogues (PXDD/Fs), and polychlorinated naphthalenes (PCNs) have been detected in dust samples from Japan.<sup>36</sup> Largely because of this recent Japanese study, PXDD/Fs and PCNs were the largest chemical groups in the household dust data set (in terms of number of unique structures). However, many of the congeners within this class are typically present at low levels in dust samples.<sup>36</sup> In recent years, an increasing number of studies have focused on industrial chemicals in settled dust including organic UV filters, organophosphorus based flame-retardants, parabens, and phthalates.

433 metabolites of the dust contaminants were proposed by MetaSite, whereas 52 of the parent dust contaminants were found to be resistant to Phase I metabolism. For these 433 dust contaminants, the most likely proposed metabolic reaction differed between the compound classes within the indoor dust data set. Aromatic compounds were commonly predicted to undergo oxidative hydroxylation of their aromatic rings. For PFASs bearing hydroxyl groups (e.g., perfluorododecanol), the hydroxyl group was often suggested to be oxidized to form a carboxylic acid. Perfluoroalkyl acids were commonly predicted to be hydroxylated at a position next to the acidic group on the alkyl chain. Substituted amines were typically reduced to the corresponding primary amines. The predicted metabolite outcomes for three compounds were compared to the results of previous experimental investigations. The software correctly predicted the major metabolites of both 2,2',4,4',5,5'-hexachlorobiphenyl (PCB153) and 2,2',4,4'-tetrabromodiphenylether (PBDE99), which are 3-OH-PCB153 and 5'-OH-PBDE99, respectively.<sup>37,38</sup> In contrast, the most abundant metabolite of 2,2',4,4'-tetrabromodiphenylether (PBDE47) in rat liver microsomes is 3-OH-PBDE47;<sup>17</sup> MetaSite predicted its major metabolite in humans to be 5-OH-PBDE47. To investigate how different CYP isoform settings influence metabolite predictions in MetaSite, we compared the results of six PCBs and two PBDEs under CYP1A1, CYP1A2, and CYP2B6 and the liver settings with experimental outcomes. The results revealed that the liver setting was most successful predicting six major metabolites correctly as compared with three, five, and four under the CYP1A1, CYP1A2, and CYP2B6 settings (Table S3). There are three potential reasons for this discrepancy: (1) human metabolic patterns differ from rat hepatic metabolism, (2) the MetaSite program accounts for the effects of metabolite accumulation, which is not an issue in microsomal incubation studies, and (3) the liver setting does not consider CYP1A and CYP2B that are known to catalyze PCB and PBDE metabolism.<sup>39</sup> These examples highlight the challenges and potential of *in silico* derived metabolic profiles but also the need for further development of these tools.

**QSAR Classification Model.** The descriptor selection strategy resulted in a final set of 14 chemical descriptors relating to physicochemical properties that are critical for interactions with TTR such as hydrophobicity, van der Waals surface area, partial charge, and numbers of hydroxyl groups and halogen atoms (Table S4). The QSAR classification models were built using kNN, LIB-SVM, PLS-DA, the selected descriptors, and the training set of 178 compounds including 70 binders and 108 nonbinders. The model built using the kNN algorithm (using a k value of 4) exhibited the best performance (Table 1), achieving the highest specificity and sensitivity values in both the internal and external validation

**Table 1. Performance of Classification Models Built Using the k Nearest Neighbor (kNN), Partial Least Squares-Discriminant Analysis (PLS-DA), and C-SVC from a Library for Support Vector Machines (LIB-SVM) Algorithm<sup>a</sup>**

modeling algorithm	cross validation			external validation		
	specificity	sensitivity	CCR <sup>b</sup>	specificity	sensitivity	CCR <sup>b</sup>
LIB-SVM	0.78	0.95	0.82	0.73	0.90	0.77
kNN	0.87	0.89	0.88	0.85	0.78	0.82
PLS-DA	0.72	0.93	0.80	0.69	0.94	0.79

<sup>a</sup>Statistics calculated according to the [Material and Methods](#) section.<sup>b</sup>Correct classification rate.

procedures. These values indicated that it performed well in identifying both true negative and true positive compounds. This model correctly classified 88% of the compounds in the training set and 82% of the validation set compounds. The model was chosen to predict whether the dust contaminants and their *in silico* derived metabolites are binders or nonbinders to TTR.

Among the 485 dust contaminants, the kNN model predicted 37 compounds as binders of TTR. Most of them belonged to three chemical classes, UV filters, PFASs, and biocides ([Table S6](#)), and 11 of these have been tested previously. They include ten true positive binders, 3,3,5,5-tetrabromobisphenol-A, triclosan, pentachlorophenol, and seven PFASs but one false positive binder, perfluorobutane-

sulfonic acid. Among the predicted nonbinders, 69 have been tested previously and only three were false negatives. The false negatives include two perfluorinated acids and 2-bis(3,5-dibromo-4-(2,3-dibromopropoxy)phenyl)propane, for which the activity of the latter could be due to contamination with its potent precursor TBBPA.<sup>40</sup>

Among the 433 potential metabolites, 230 were classified as potential TTR binders ([Table S7](#)). The percentage of binders in the metabolites data set was 53.1% whereas that in the parent data set was only 7.6%. This indicates the profound impact of metabolism on TTR interaction. The increase in the proportion of predicted binders was primarily due to bioactivation of the halogenated aromatic compounds that dominate the dust chemical data set. During metabolic processing, these compounds are prone to hydroxylation of their aromatic rings, which is known to favor TTR binding.<sup>16,17</sup> Only a minor share of TTR binding metabolites was derived from UV filters (10) or PFASs (7).

On the basis of the model's defined AD, 39 moderate and 22 severe outliers were identified among the parent dust chemicals along with 15 moderate and 4 severe outlying metabolites ([Table S5](#)). The outliers mainly belong to four groups: various volatile organics, organotin, organosiloxanes, and PFASs. Except for the PFASs, these classes of chemicals were not represented in the training set, and thus, the model was not tailored for these. Concerning the PFASs, the outliers include those with long perfluorinated chains or functionalities that

**Table 2. Classification of Selected Compounds as Competitive Binders (B) or Nonbinders (NB) from the k Nearest Neighbor Model and Experimentally Determined IC<sub>50</sub> Values<sup>a</sup>**

chemical	CAS No.	chemical class	prediction	IC <sub>50</sub> (μM) <sup>c</sup>	REP
thyroxine (T4) <sup>b</sup>	7488-70-2			0.070–0.110 <sup>d</sup>	1
perfluorohexylphosphonic acid (C6-PFPA)	40143-76-8	PFAS	B	NR	
perfluoroheptanesulfonic acid (PFHpS) <sup>b</sup>	375-92-8	PFAS	B	0.64	0.17
2,4,2',4'-tetrahydroxybenzophenone (BP2) <sup>b</sup>	131-55-5	UV filter	B	0.62	0.18
2-(2'-hydroxy-3'-tert-butyl-5'-methylphenyl)-5-chlorobenzotriazole (Tinuvin 326)	3896-11-5	UV filter	B	NR	
2-(2-hydroxy-3,5-ditert-butylphenyl)-5-chlorobenzotriazole (Tinuvin 327)	3864-99-1	UV filter	B	NR	
2,4,5-trichlorophenoxyacetic acid (2,4,5-T) <sup>b</sup>	93-76-5	biocide	B	10	0.0066
3,5,6-trichloro-2-pyridinol (3,5,6-TC2P) <sup>b</sup>	6515-38-4	biocide	B	2.9	0.039
2-tert-butyl-4-(2,4-dichloro-5-isopropoxyphenyl)-5-oxo-1,3,4-oxadiazoline (Oxadiazon)	19666-30-9	biocide	B	NR	
1-[(2,4-dichlorophenyl)aminocarbonyl]-1-cyclopropanecarboxylic acid (cyclanilide)	113136-77-9	biocide	B	NR	
3,6-dichloro-2-methoxybenzoic acid (dicamba)	1918-00-9	biocide	B	NR	
4-nitrophenol	100-02-7	biocide	B	NR	
mono-[2-(perfluorohexyl)ethyl] phosphate (6:2 monoPAP)	57678-01-0	PFAS	NB	NR	
mono [2-(perfluorooctyl)ethyl] phosphate (8:2 monoPAP)	57678-03-2	PFAS	NB	NR	
sodium bis(1H,1H,2H,2H-perfluorodecyl)phosphate (6:2 PAP)	678-41-1	PFAS	NB	NR	
sodium bis(1H,1H,2H,2H-perfluorooctyl)phosphate (8:2 PAP)	57677-95-9	PFAS	NB	NR	
perfluorodecylphosphonic acid (C10-PFPA)	52299-26-0	PFAS	NB	23	0.0030
tris(isobutyl) phosphate (TIBP)	126-71-6	organophosphate	NB	NR	
tris(2-butoxyethyl) phosphate (TBOEP)	78-51-3	organophosphate	NB	NR	
tris(1-chloro-2-propyl) phosphate (TCIPP)	13674-84-5	organophosphate	NB	NR	
methyl paraben (MP)	99-76-3	paraben	NB	NR	
ethyl paraben (EP)	120-47-8	paraben	NB	138	0.00053
propyl paraben (PP)	94-13-3	paraben	NB	19	0.0038
butyl paraben (BP)	94-26-8	paraben	NB	43	0.0017

<sup>a</sup>Chemicals are given with abbreviations, selected trade names, Chemical Abstracts Service numbers (CAS No.), and chemical class ([Table S1](#)).<sup>b</sup>Selected for molecular docking studies. <sup>c</sup>NR refers to no response (i.e., <20% inhibited T4-binding) at 10 μM. <sup>d</sup>IC<sub>50</sub>-interval of T4 derived from individual runs in this study.

were not included in the training set, such as phosphonic acids, sulfonates, fluorotelomer alcohols, and phosphates.

**TTR Binding Assay.** We selected 23 parent dust contaminants (11 predicted binders and 12 predicted nonbinders) for testing in the radio-ligand TTR binding assay with a focus on studying nontested indoor dust contaminants and identifying new potential THDCs. The predicted binders include PFASs, UV filters, and biocides, and the predicted nonbinders were PFASs, organophosphates, and parabens (Table 2). No metabolites were selected for testing as very few are commercially available as standards. According to the assay results, 4 out of 11 predicted binders exhibited strong TTR interaction ( $IC_{50}$  values  $\leq 10 \mu M$ ) whereas all 12 predicted nonbinders showed no or weak TTR binding potency ( $IC_{50} > 10 \mu M$ ). The binding activities of all tested compounds are listed in Table 2, and their dose–response curves are shown in Figure 2. In addition, it was noted that the

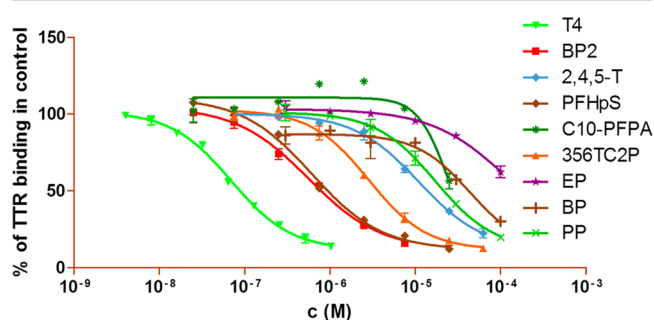


**Figure 2.** Dose–response curves for the binding of selected ligands to transthyretin (TTR). Thyroxine (T4) was used as positive control, remaining compounds are abbreviated according to Table 2.

model seems capable of predicting metabolites as assessed by four hydroxylated PCBs and five hydroxylated PBDEs: 5-OH PCB77, 4-OH PCB107, 4'-OH PCB172, 4-OH PCB187, 4'-OH PBDE17, 3'-OH PBDE28, 5-OH PBDE47, 4'-OH PBDE49, and 3-OH PBDE154 (that were all predicted correctly as active).<sup>41–43</sup>

Among the four confirmed TTR binders, the most potent one was 2,2',4,4'-tetrahydroxybenzophenone (BP2) that is widely used, e.g., in personal care products to protect skin and hair from UV irradiation. It has been found in household dust from the US and East Asian countries, but also in sewage sludge samples from China and female urine samples.<sup>44–46</sup> Moreover, it has been reported to inhibit human thyroid peroxidase and to induce endometriosis.<sup>46,47</sup> It also showed weak antithyroidal activity in both rodent studies and an amphibian metamorphosis assay.<sup>48</sup> Perfluoroheptanesulfonic acid (PFHpS) was identified as the second strongest TTR binder in this study. This compound has been found in the blood plasma of pregnant mothers from coastal populations in Norway.<sup>49,50</sup> To our knowledge, its thyroid effects have not previously been investigated, even though the result is in agreement with the TTR binding potency measured for the related perfluorooctanesulfonic acid (PFOS) and perfluorohexanesulfonic acid (PFHxS).<sup>4</sup> The other two TTR binders were the biocides 3,5,6-trichloro-2-pyridinol (3,5,6-TC2P) and 2,4,5-trichlorophenoxyacetic acid (2,4,5-T). Both have been found in homes and daycare products in North Carolina, USA.<sup>51,52</sup> 3,5,6-TC2P is known to increase T4 levels and reduce thyroid-stimulating hormone levels in men.<sup>53</sup> Additionally, children from both Spain and Australia have been reported to be

exposed to the compound.<sup>54,55</sup> 2,4,5-T (a major ingredient of the defoliant Agent Orange) has been linked to the development of hypothyroidism and prostate and skin cancer.<sup>56–58</sup>

A number of false positives were identified and these may be misclassified as (1) there are more nonbinders (108) than binders (70) in the training set and (2) the majority of binders (73%) in the training set belong to only three compound groups, i.e., OH-PCBs, OH-PBDEs, and PFAS, whereas the nonbinders are more structurally diverse. This means that the model is less well trained covering a narrower chemical domain of binders as compared with nonbinders and may hence be less capable of identifying true positives. The misclassification of 2-(2'-hydroxy-3'-tert-butyl-5'-methylphenyl)-5-chlorobenzotriazole (Tinuvin 326) and 2-(2-hydroxy-3,5-ditert-butylphenyl)-5-chlorobenzotriazole (Tinuvin 327) may be due to their chlorine atom and hydroxyl-group on aromatic rings which are chemical functionalities of common binders. Possibly the bulky butyl group adjacent to the hydroxyl-group hinders interactions at TTR for these compounds and the model is not trained with structurally similar chemicals. Another potential reason for misclassification could be that the model was developed on the neutral form of the ligand whereas some of the compounds are weak acids and may dissociate in the assay (pH = 8.0), such as 1-[(2,4-dichlorophenyl)aminocarbonyl]-1-cyclopropanecarboxylic acid ( $pK_a = 3.39 \pm 0.20$ ) and 3,6-dichloro-2-methoxybenzoic acid ( $pK_a = 2.40 \pm 0.25$ ) ( $pK_a$  values from SciFinder (<http://www.cas.org/products/scifinder>)).

Four compounds were correctly classified as nonbinders (i.e.,  $IC_{50} > 10 \mu M$ ), but exhibited very weak affinity at high concentrations including parabens and a PFAS (Table 2). Three parabens are of particular environmental importance as they are widely used as antimicrobial preservatives in personal care products, cosmetics, and pharmaceuticals. EU regulations also permit the use of methylparaben (MP), ethylparaben (EP), and propylparaben (PP) as food preservatives.<sup>59</sup> High levels of these chemicals were found in urine samples from Swedish mothers and their children, as well as in biota.<sup>60,61</sup> A recent study has reported associations between parabens and TH levels in females but not males, which might be related to gender differences in use of personal care products.<sup>62</sup> The fourth compound with weak TTR binding affinity at high concentrations, perfluorodecylphosphonic acid, has been detected in household dust from Vancouver, Canada,<sup>63</sup> for which, to our knowledge, no data on TH related effects are reported.

**Docking Study of the Confirmed TTR Binders.** The four confirmed TTR binders, BP2, 3,5,6-TC2P, 2,4,5-T, and PFHpS, together with the endogenous ligand T4 and the coligand Tafamidis, (Table 2) were docked into the ligand-binding pocket. The selected docking poses of the TTR binders and T4 revealed their interactions with the tetramer (Figure 3B). The root-mean-square-deviation between the Tafamidis docking and crystal pose was 0.006 Å, which indicated that the molecular docking was able to reproduce its actual binding pose. Crystal data and our docking studies suggested that T4 interacts with TTR via Lys15 B and Glu54 B,<sup>64</sup> which is different from the identified exogenous TTR binders. The difference may be due to the smaller molecular size of the xenobiotics allowing them to interact with residues deeper in the binding pocket. BP2 shared a similar binding pose with the OH-PCB derivative, 3,3',5,5'-tetrachloro-4,4'-biphenyldiol, including interaction with Ser117A that is crucial for binding to



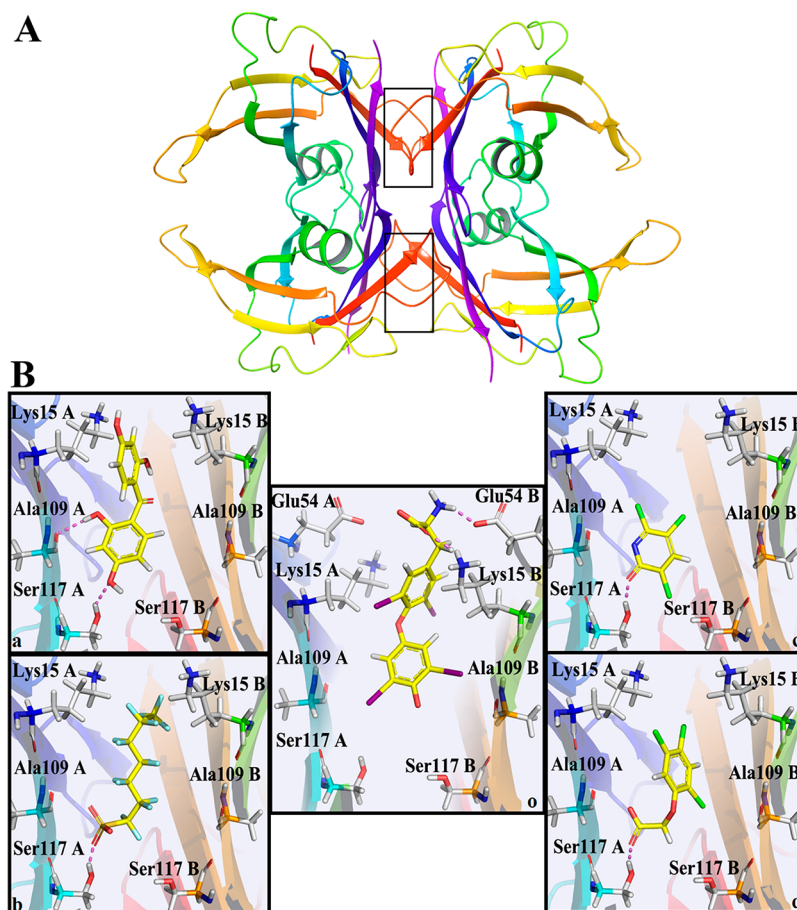


**Figure 3.** (A) Hormone binding sites in the transthyretin (TTR) homotetramer and (B) proposed orientations of binding between human transthyretin and selected ligands, with hydrogen bonds indicated using pink dashed lines: (a) 2,2',4,4'-tetrahydroxybenzophenone, (b) perfluoroheptanesulfonic acid, (c) 3,5,6-trichloro-2-pyridinol, (d) 2,4,5-trichlorophenoxyacetic acid, and (e) L-thyroxine (T4).

TTR of the PCB derivative.<sup>65</sup> BP2 formed a second hydrogen bond with Ala109A, which may explain its relatively high potency. The docking pose of 3,5,6-TC2P was similar to the crystal pose of 2,4-dinitrophenol, and they interacted as well with Ser117A.<sup>66</sup> It has also been shown that pentabromophenol interacts with Ser117A but also Lys15A.<sup>67</sup> These interactions were mediated through water-bridged hydrogen bonds that were not considered by the applied molecular docking protocol. 2,4,5-T was shown to bind to TTR in a similar mode as the crystal structure of 3-[(9H-fluoren-9-ylideneamino)oxy]-propanoic acid.<sup>68</sup> The carboxylic groups of these compounds interact with Ser117A of the TTR complex. No structurally similar coligand was found for PFHpS, and future crystallization studies of PFAS representatives are warranted to increase our understanding on their interactions with TTR.

To identify new THDCs, we developed a QSAR classification model using kNN with a correct classification rate of 82% of the external validation set. The model was applied to an in-house database including 485 dust contaminants and their 433 *in silico* derived metabolites. The model predicted 37 (7.6%) dust contaminants and 230 (53.1%) dust metabolites as potential TTR binders. These outcomes stress the importance of metabolic activation for binding to TTR. Twenty-three nontested household dust contaminants were tested in a radio-ligand TTR binding assay, and among these, four new compounds, BP2, 3,5,6-TC2P, 2,4,5-T, and PFHpS, were confirmed as TTR binders with  $IC_{50}$  values  $\leq 10 \mu M$ .

Molecular docking studies revealed that the four TTR binders interacted with TTR via the Ser117A residue that is known to be critical for strong interaction. Organic contaminants in household dust could disturb several pathways of the thyroid hormone regulation, and in this study, we focused on binding to the transporter TTR. Further studies are warranted on the identified binders covering other possible thyroid related mechanisms of action and including the significance of metabolism.

## ■ ASSOCIATED CONTENT

### 📄 Supporting Information

The Supporting Information is available free of charge on the ACS Publications website at DOI: 10.1021/acs.est.5b01742.

Details of the compounds tested in the bioassay, the TTR data set, the indoor dust data set, and the chemical compositions of indoor dust; descriptions of the subset partitioning method and modeling algorithms; descriptions of MI-DSE method and definitions of selected descriptors and their MI-DSE values (PDF)

## ■ AUTHOR INFORMATION

### Corresponding Author

\*E-mail: [patrik.andersson@umu.se](mailto:patrik.andersson@umu.se); phone: +46-90-786-5266.

### Notes

The authors declare no competing financial interest.

## ACKNOWLEDGMENTS

This study was financed by the MiSSE project through grants from the Swedish Research Council for the Environment, Agricultural Sciences and Spatial Planning (Formas) (210-2012-131) and by the Swedish Research Council (VR) (521-2011-6427).

## REFERENCES

- (1) Murk, A. J.; Rijntjes, E.; Blaauboer, B. J.; Clewell, R.; Crofton, K. M.; Dingemans, M. M.; Furlow, J. D.; Kavlock, R.; Kohrle, J.; Opitz, R.; Traas, T.; Visser, T. J.; Xia, M.; Gutleb, A. C. Mechanism-based testing strategy using in vitro approaches for identification of thyroid hormone disrupting chemicals. *Toxicol. In Vitro* **2013**, *27* (4), 1320–1346.
- (2) Lopez-Espinosa, M. J.; Mondal, D.; Armstrong, B.; Bloom, M. S.; Fletcher, T. Thyroid function and perfluoroalkyl acids in children living near a chemical plant. *Environ. Health Perspect* **2012**, *120* (7), 1036–41.
- (3) Meerts, I. A.; van Zanden, J. J.; Luijckx, E. A.; van Leeuwen-Bol, L.; Marsh, G.; Jakobsson, E.; Bergman, A.; Brouwer, A. Potent competitive interactions of some brominated flame retardants and related compounds with human transthyretin in vitro. *Toxicol. Sci.* **2000**, *56* (1), 95–104.
- (4) Weiss, J. M.; Andersson, P. L.; Lamoree, M. H.; Leonards, P. E.; van Leeuwen, S. P.; Hamers, T. Competitive binding of poly- and perfluorinated compounds to the thyroid hormone transport protein transthyretin. *Toxicol. Sci.* **2009**, *109* (2), 206–16.
- (5) Haddow, J. E.; Palomaki, G. E.; Allan, W. C.; Williams, J. R.; Knight, G. J.; Gagnon, J.; O’Heir, C. E.; Mitchell, M. L.; Hermos, R. J.; Waisbren, S. E.; Faix, J. D.; Klein, R. Z. Maternal thyroid deficiency during pregnancy and subsequent neuropsychological development of the child. *N. Engl. J. Med.* **1999**, *341* (8), 549–555.
- (6) de Jong, F. J.; Masaki, K.; Chen, H.; Remaley, A. T.; Breteler, M. M.; Petrovitch, H.; White, L. R.; Launer, L. J. Thyroid function, the risk of dementia and neuropathologic changes: the Honolulu-Asia aging study. *Neurobiol. Aging* **2009**, *30* (4), 600–6.
- (7) Tan, Z. S.; Vasan, R. S. Thyroid function and Alzheimer’s disease. *J. Alzheimers Dis.* **2009**, *16* (3), 503–507.
- (8) Meerts, I. A.; Assink, Y.; Cuijn, P. H.; Van Den Berg, J. H.; Weijers, B. M.; Bergman, A.; Koeman, J. H.; Brouwer, A. Placental transfer of a hydroxylated polychlorinated biphenyl and effects on fetal and maternal thyroid hormone homeostasis in the rat. *Toxicol. Sci.* **2002**, *68* (2), 361–371.
- (9) Zhou, T.; Taylor, M. M.; DeVito, M. J.; Crofton, K. M. Developmental exposure to brominated diphenyl ethers results in thyroid hormone disruption. *Toxicol. Sci.* **2002**, *66* (1), 105–116.
- (10) Jones-Otazo, H. A.; Clarke, J. P.; Diamond, M. L.; Archbold, J. A.; Ferguson, G.; Harner, T.; Richardson, G. M.; Ryan, J. J.; Wilford, B. Is house dust the missing exposure pathway for PBDEs? An analysis of the urban fate and human exposure to PBDEs. *Environ. Sci. Technol.* **2005**, *39* (14), 5121–30.
- (11) Fromme, H.; Lahrz, T.; Kraft, M.; Fembacher, L.; Mach, C.; Dietrich, S.; Burkhardt, R.; Volkel, W.; Goen, T. Organophosphate flame retardants and plasticizers in the air and dust in German daycare centers and human biomonitoring in visiting children (LUPE 3). *Environ. Int.* **2014**, *71*, 158–63.
- (12) US EPA. *Exposure Factors Handbook (1997 Final Report)*; US EPA: Washington, DC, 1997.
- (13) Liroy, P. J.; Freeman, N. C.; Millette, J. R. Dust: a metric for use in residential and building exposure assessment and source characterization. *Environ. Health Perspect* **2002**, *110* (10), 969–83.
- (14) Mercier, F.; Glorenne, P.; Thomas, O.; Le Bot, B. Organic contamination of settled house dust, a review for exposure assessment purposes. *Environ. Sci. Technol.* **2011**, *45* (16), 6716–6727.
- (15) Hakk, H.; Letcher, R. J. Metabolism in the toxicokinetics and fate of brominated flame retardants—a review. *Environ. Int.* **2003**, *29* (6), 801–828.
- (16) Ucan-Marín, F.; Arukwe, A.; Mortensen, A.; Gabrielsen, G. W.; Fox, G. A.; Letcher, R. J. Recombinant transthyretin purification and competitive binding with organohalogen compounds in two gull species (*Larus argentatus* and *Larus hyperboreus*). *Toxicol. Sci.* **2009**, *107* (2), 440–450.
- (17) Hamers, T.; Kamstra, J. H.; Sonneveld, E.; Murk, A. J.; Visser, T. J.; Van Velzen, M. J.; Brouwer, A.; Bergman, A. Biotransformation of brominated flame retardants into potentially endocrine-disrupting metabolites, with special attention to 2,2’,4,4’-tetrabromodiphenyl ether (BDE-47). *Mol. Nutr. Food Res.* **2008**, *52* (2), 284–98.
- (18) Ren, X. M.; Guo, L. H. Assessment of the binding of hydroxylated polybrominated diphenyl ethers to thyroid hormone transport proteins using a site-specific fluorescence probe. *Environ. Sci. Technol.* **2012**, *46* (8), 4633–40.
- (19) Lans, M. C.; Klasson-Wehler, E.; Willemsen, M.; Meussen, E.; Safe, S.; Brouwer, A. Structure-dependent, competitive interaction of hydroxy-polychlorobiphenyls, -dibenzo-p-dioxins and -dibenzofurans with human transthyretin. *Chem.-Biol. Interact.* **1993**, *88* (1), 7–21.
- (20) Hovander, L.; Linderholm, L.; Athanasiadou, M.; Athanassiadis, I.; Bignert, A.; Fangstrom, B.; Kocan, A.; Petrik, J.; Trnovec, T.; Bergman, A. Levels of PCBs and their metabolites in the serum of residents of a highly contaminated area in eastern Slovakia. *Environ. Sci. Technol.* **2006**, *40* (12), 3696–703.
- (21) Athanasiadou, M.; Cuadra, S. N.; Marsh, G.; Bergman, A.; Jakobsson, K. Polybrominated diphenyl ethers (PBDEs) and bioaccumulative hydroxylated PBDE metabolites in young humans from Managua, Nicaragua. *Environ. Health Perspect.* **2008**, *116* (3), 400–408.
- (22) Mansouri, K.; Ringsted, T.; Ballabio, D.; Todeschini, R.; Consonni, V. Quantitative structure-activity relationship models for ready biodegradability of chemicals. *J. Chem. Inf. Model.* **2013**, *53* (4), 867–78.
- (23) von der Ohe, P. C.; Kuhne, R.; Ebert, R. U.; Altenburger, R.; Liess, M.; Schuurmann, G. Structural alerts—a new classification model to discriminate excess toxicity from narcotic effect levels of organic compounds in the acute daphnid assay. *Chem. Res. Toxicol.* **2005**, *18* (3), 536–55.
- (24) Singh, N.; Chaudhury, S.; Liu, R.; AbdulHameed, M. D.; Tawa, G.; Wallqvist, A. QSAR classification model for antibacterial compounds and its use in virtual screening. *J. Chem. Inf. Model.* **2012**, *52* (10), 2559–69.
- (25) Weiss, J. M.; Andersson, P. L.; Zhang, J.; Simon, E.; Leonards, P. E.; Hamers, T.; Lamoree, M. H. Tracing thyroid hormone-disrupting compounds: database compilation and structure-activity evaluation for an effect-directed analysis of sediment. *Anal. Bioanal. Chem.* **2015**, *407*, 5625–5634.
- (26) Cruciani, G.; Carosati, E.; De Boeck, B.; Ethirajulu, K.; Mackie, C.; Howe, T.; Vianello, R. MetaSite: understanding metabolism in human cytochromes from the perspective of the chemist. *J. Med. Chem.* **2005**, *48* (22), 6970–9.
- (27) JChem 6.2.0, Feb 10, 2014, ChemAxon (<http://www.chemaxon.com>), 2014 (accession date: Feb 10, 2014).
- (28) Molecular Operating Environment (MOE), 2013.08; Chemical Computing Group Inc.: Montreal, QC, Canada, 2015.
- (29) Daszykowski, M.; Walczak, B.; Massart, D. L. Representative subset selection. *Anal. Chim. Acta* **2002**, *468* (1), 91–103.
- (30) Wassermann, A. M.; Nisius, B.; Vogt, M.; Bajorath, J. Identification of descriptors capturing compound class-specific features by mutual information analysis. *J. Chem. Inf. Model.* **2010**, *50* (11), 1935–40.
- (31) Ballabio, D.; Consonni, V. Classification tools in chemistry. Part 1: linear models. PLS-DA. *Anal. Methods* **2013**, *5* (16), 3790–3798.
- (32) Chang, C. C.; Lin, C. J. *ACM Transactions on Intelligent Systems and Technology (TIST)*; Volume 2, Issue 3, April, 2011, Article No. 27, 2:27:1–27:27 <http://dl.acm.org/citation.cfm?id=1961199>.
- (33) Protein Preparation Wizard 2014-3; Schrodinger, LLC: New York, NY, 2014.
- (34) LigPrep, Version 2.9; Schrodinger, LLC: New York, NY, 2014.
- (35) Glide, Version 6.3; Schrodinger, LLC: New York, NY, 2014.



- (36) Suzuki, G.; Someya, M.; Takahashi, S.; Tanabe, S.; Sakai, S.; Takigami, H. Dioxin-like activity in Japanese indoor dusts evaluated by means of in vitro bioassay and instrumental analysis: brominated dibenzofurans are an important contributor. *Environ. Sci. Technol.* **2010**, *44* (21), 8330–6.
- (37) Erratico, C. A.; Szeitz, A.; Bandiera, S. M. Oxidative metabolism of BDE-99 by human liver microsomes: predominant role of CYP2B6. *Toxicol. Sci.* **2012**, *129* (2), 280–92.
- (38) Norback, D. H.; Mack, E.; Reddy, G.; Britt, J.; Hsia, M. T. Metabolism and biliary excretion of 2,4,5,2',4',5'-hexachlorobiphenyl in the rhesus monkey (*Macaca mulatta*). *Res. Commun. Chem. Pathol. Pharmacol.* **1981**, *32* (1), 71–85.
- (39) Grimm, F. A.; Hu, D.; Kania-Korwel, I.; Lehmler, H. J.; Ludewig, G.; Hornbuckle, K. C.; Duffel, M. W.; Bergman, A.; Robertson, L. W. Metabolism and metabolites of polychlorinated biphenyls. *Crit. Rev. Toxicol.* **2015**, *45* (3), 245–72.
- (40) Hamers, T.; Kamstra, J. H.; Sonneveld, E.; Murk, A. J.; Kester, M. H.; Andersson, P. L.; Legler, J.; Brouwer, A. In vitro profiling of the endocrine-disrupting potency of brominated flame retardants. *Toxicol. Sci.* **2006**, *92* (1), 157–173.
- (41) Cao, J.; Lin, Y.; Guo, L. H.; Zhang, A. Q.; Wei, Y.; Yang, Y. Structure-based investigation on the binding interaction of hydroxylated polybrominated diphenyl ethers with thyroxine transport proteins. *Toxicology* **2010**, *277* (1–3), 20–8.
- (42) Darnerud, P. O.; Morse, D.; Klasson-Wehler, E.; Brouwer, A. Binding of a 3,3', 4,4'-tetrachlorobiphenyl (CB-77) metabolite to fetal transthyretin and effects on fetal thyroid hormone levels in mice. *Toxicology* **1996**, *106* (1–3), 105–14.
- (43) Simon, E.; Bytingsvik, J.; Jonker, W.; Leonards, P. E.; de Boer, J.; Jenssen, B. M.; Lie, E.; Aars, J.; Hamers, T.; Lamoree, M. H. Blood plasma sample preparation method for the assessment of thyroid hormone-disrupting potency in effect-directed analysis. *Environ. Sci. Technol.* **2011**, *45* (18), 7936–44.
- (44) Wang, L.; Asimakopoulos, A. G.; Moon, H. B.; Nakata, H.; Kannan, K. Benzotriazole, benzothiazole, and benzophenone compounds in indoor dust from the United States and East Asian countries. *Environ. Sci. Technol.* **2013**, *47* (9), 4752–9.
- (45) Zhang, Z.; Ren, N.; Li, Y. F.; Kunisue, T.; Gao, D.; Kannan, K. Determination of benzotriazole and benzophenone UV filters in sediment and sewage sludge. *Environ. Sci. Technol.* **2011**, *45* (9), 3909–16.
- (46) Kunisue, T.; Chen, Z.; Buck Louis, G. M.; Sundaram, R.; Hediger, M. L.; Sun, L.; Kannan, K. Urinary concentrations of benzophenone-type UV filters in U.S. women and their association with endometriosis. *Environ. Sci. Technol.* **2012**, *46* (8), 4624–32.
- (47) Schmutzler, C.; Bacinski, A.; Gotthardt, I.; Huhne, K.; Ambrügger, P.; Klammer, H.; Schlecht, C.; Hoang-Vu, C.; Gruters, A.; Wuttke, W.; Jarry, H.; Kohrle, J. The ultraviolet filter benzophenone 2 interferes with the thyroid hormone axis in rats and is a potent in vitro inhibitor of human recombinant thyroid peroxidase. *Endocrinology* **2007**, *148* (6), 2835–44.
- (48) OECD. Report of the validation of the amphibian metamorphosis assay (Phase 3); ENV/JM/MONO(2008)18; IOMC: Paris, 2008.
- (49) Starling, A. P.; Engel, S. M.; Whitworth, K. W.; Richardson, D. B.; Stuebe, A. M.; Daniels, J. L.; Haug, L. S.; Eggesbo, M.; Becher, G.; Sabareedzovic, A.; Thomsen, C.; Wilson, R. E.; Travlos, G. S.; Hoppin, J. A.; Baird, D. D.; Longnecker, M. P. Perfluoroalkyl substances and lipid concentrations in plasma during pregnancy among women in the Norwegian Mother and Child Cohort Study. *Environ. Int.* **2014**, *62*, 104–112.
- (50) Rylander, C.; Brustad, M.; Falk, H.; Sandanger, T. M. Dietary predictors and plasma concentrations of perfluorinated compounds in a coastal population from northern Norway. *J. Environ. Public Health* **2009**, *2009*, 268219.
- (51) Morgan, M. K.; Sheldon, L. S.; Croghan, C. W.; Jones, P. A.; Robertson, G. L.; Chuang, J. C.; Wilson, N. K.; Lyu, C. W. Exposures of preschool children to chlorpyrifos and its degradation product 3,5,6-trichloro-2-pyridinol in their everyday environments. *J. Exposure Anal. Environ. Epidemiol.* **2005**, *15* (4), 297–309.
- (52) Morgan, M. K.; Wilson, N. K.; Chuang, J. C. Exposures of 129 preschool children to organochlorines, organophosphates, pyrethroids, and acid herbicides at their homes and daycares in North Carolina. *Int. J. Environ. Res. Public Health* **2014**, *11* (4), 3743–64.
- (53) Fortenberry, G. Z.; Hu, H.; Turyk, M.; Barr, D. B.; Meeker, J. D. Association between urinary 3, 5, 6-trichloro-2-pyridinol, a metabolite of chlorpyrifos and chlorpyrifos-methyl, and serum T4 and TSH in NHANES 1999–2002. *Sci. Total Environ.* **2012**, *424*, 351–5.
- (54) Roca, M.; Miralles-Marco, A.; Ferre, J.; Perez, R.; Yusa, V. Biomonitoring exposure assessment to contemporary pesticides in a school children population of Spain. *Environ. Res.* **2014**, *131*, 77–85.
- (55) Babina, K.; Dollard, M.; Pilotto, L.; Edwards, J. W. Environmental exposure to organophosphorus and pyrethroid pesticides in South Australian preschool children: a cross sectional study. *Environ. Int.* **2012**, *48*, 109–20.
- (56) Ansbaugh, N.; Shannon, J.; Mori, M.; Farris, P. E.; Garzotto, M. Agent Orange as a risk factor for high-grade prostate cancer. *Cancer* **2013**, *119* (13), 2399–404.
- (57) Clemens, M. W.; Kochuba, A. L.; Carter, M. E.; Han, K.; Liu, J.; Evans, K. Association between Agent Orange exposure and non-melanotic invasive skin cancer: a pilot study. *Plast Reconstr Surg* **2014**, *133* (2), 432–7.
- (58) Goldner, W. S.; Sandler, D. P.; Yu, F.; Shostrom, V.; Hoppin, J. A.; Kamel, F.; LeVan, T. D. Hypothyroidism and pesticide use among male private pesticide applicators in the agricultural health study. *J. Occup. Environ. Med.* **2013**, *55* (10), 1171–8.
- (59) European Parliament and Council Directive No 95/2/EC of 20 February 1995 on Food Additives Other than Colours and Sweeteners; European Union: Brussels, Belgium, 1995.
- (60) Larsson, K.; Ljung Bjorklund, K.; Palm, B.; Wennberg, M.; Kaj, L.; Lindh, C. H.; Jonsson, B. A.; Berglund, M. Exposure determinants of phthalates, parabens, bisphenol A and triclosan in Swedish mothers and their children. *Environ. Int.* **2014**, *73*, 323–33.
- (61) Bledzka, D.; Gromadzinska, J.; Wasowicz, W. Parabens. From environmental studies to human health. *Environ. Int.* **2014**, *67*, 27–42.
- (62) Koeppe, E. S.; Ferguson, K. K.; Colacino, J. A.; Meeker, J. D. Relationship between urinary triclosan and paraben concentrations and serum thyroid measures in NHANES 2007–2008. *Sci. Total Environ.* **2013**, *445–446*, 299–305.
- (63) De Silva, A. O.; Allard, C. N.; Spencer, C.; Webster, G. M.; Shoeib, M. Phosphorus-containing fluorinated organics: polyfluoroalkyl phosphoric acid diesters (diPAPs), perfluorophosphonates (PFPAAs), and perfluorophosphinates (PFPIAs) in residential indoor dust. *Environ. Sci. Technol.* **2012**, *46* (22), 12575–82.
- (64) Wojtczak, A.; Neumann, P.; Cody, V. Structure of a new polymorphic monoclinic form of human transthyretin at 3 Å resolution reveals a mixed complex between unliganded and T4-bound tetramers of TTR. *Acta Crystallogr., Sect. D: Biol. Crystallogr.* **2001**, *57*, 957–967.
- (65) Purkey, H. E.; Palaninathan, S. K.; Kent, K. C.; Smith, C.; Safe, S. H.; Sacchettini, J. C.; Kelly, J. W. Hydroxylated polychlorinated biphenyls selectively bind transthyretin in blood and inhibit amyloidogenesis: rationalizing rodent PCB toxicity. *Chem. Biol.* **2004**, *11* (12), 1719–28.
- (66) Morais-de-Sa, E.; Neto-Silva, R. M.; Pereira, P. J.; Saraiva, M. J.; Damas, A. M. The binding of 2,4-dinitrophenol to wild-type and amyloidogenic transthyretin. *Acta Crystallogr., Sect. D: Biol. Crystallogr.* **2006**, *62*, 512–519.
- (67) Ghosh, M.; Meerts, I. A.; Cook, A.; Bergman, A.; Brouwer, A.; Johnson, L. N. Structure of human transthyretin complexed with bromophenols: a new mode of binding. *Acta Crystallogr., Sect. D: Biol. Crystallogr.* **2000**, *56*, 1085–1095.
- (68) Palaninathan, S. K.; Mohamedmohideen, N. N.; Orlandini, E.; Ortore, G.; Nencetti, S.; Lapucci, A.; Rossello, A.; Freundlich, J. S.; Sacchettini, J. C. Novel transthyretin amyloid fibril formation inhibitors: synthesis, biological evaluation, and X-ray structural analysis. *PLoS One* **2009**, *4* (7), e6290.